

Phase diagram of a frustrated asymmetric ferromagnetic spin ladder

Lihua Pan

School of Physics Science and Technology, Yangzhou University, Yangzhou
225002, China

Depeng Zhang

School of Physics Science and Technology, Yangzhou University, Yangzhou
225002, China

Hsiang-Hsuan Hung

Department of Physics, The University of Texas at Austin, Austin, Texas 78712, USA

Yong-Jun Liu

School of Physics Science and Technology, Yangzhou University, Yangzhou
225002, China

Abstract. We perform a systematic investigation on the ground state of an asymmetric two-leg spin ladder (where exchange couplings of the legs are unequal) with ferromagnetic (FM) nearest-neighbor interaction and diagonal anti-ferromagnetic frustration using the Density Matrix Renormalization Group (DMRG) method. When the ladder is strongly asymmetric with moderate frustration, a magnetic canted state is observed between an FM state and a singlet dimerized state. The phase boundaries are dependent on the asymmetric strength. On the other hand, when the asymmetric strength is intermediate, a so-called spin-stripe state (spins align parallel on same legs, but antiparallel on rungs) is discovered, and the system experiences a first-order phase transition from the FM state to the spin-stripe state upon increasing frustration. We present numerical evidence to interpret the phase diagram in terms of frustration and the asymmetric strength.

1. Introduction

Frustrated quantum magnetism in low dimensions has received considerable attention in recent decades. The exotic magnetic behavior arises from frustrated geometry, such as triangular lattices and Kagóme lattices, which usually offer a large degeneracy in the thermodynamic limit[1]. In quantum limit, this is relevant to the quantum spin liquids. Recently, $\text{ZnCu}_3(\text{OD})_6\text{Cl}_2$, also called herbertsmithite, was experimentally identified as a promising spin liquids and is modeled as the spin-1/2 kagóme-lattice antiferromagnet[2]. Another indication for frustrated magnetism is in the spin-1/2 antiferromagnetic (AF) Heisenberg model on a two-dimensional square lattice. Without frustration, the ground state is the Néel ordering[3, 4] and the model provides a description of the parents of La_2CuO_4 [4, 5]. With next-nearest-neighbor (NNN) AF exchange, however, the other magnetic collinear state will be triggered to compete with the Néel state. As the NNN exchange is at the same order of the NN one, the ground state is magnetically disordered[6, 7, 8], and recently has been identified to have a character of the spin liquids state[9]. The liquid state may be relevant to high-temperature superconductors[10, 11].

The exotic state is however difficult to be determined without any unambiguity. Theoretically the many-body effect prevents us against directly studying it, and numerically the frustrated spin systems suffer the minus sign problems, so the quantum Monte Carlo is unable to accurately capture the behavior. The spin ladder instead provides another route to study the physics since a ladder plays a role crossover from one dimensions and two dimensions[12, 13, 14]. The frustrated two-leg spin ladders have been intensively investigated during the decade[15, 16, 17, 18, 19, 20, 21, 22, 23, 24, 25]. Without frustrated NNN AF exchange, the ground state is singlet with a finite spin gap[12, 26]. In the large NNN AF couplings limit, the ladder topologically behaves as a spin-1 chain[17]. In addition, it has been argued that there exists an intermediate state, the columnar dimer state, in the moderate frustration regime[16, 21, 23]. This indicates that even in a two-leg ladder frustrated magnetism can provide rich phase diagrams.

Recently, the one-dimensional Heisenberg model with ferromagnetic (FM) NN interaction with AF NNN exchange (represented as the zigzag ladder) has also been frequently mentioned[27, 28, 29, 30, 31, 32, 33, 34, 35, 36, 37] since experimentally the corresponding materials are discovered, including the edge-sharing CuO_2 chains NaCu_2O_2 [38], quasi-onedimensional helimagnet LiCuVO_4 [39], and powder curprate $\text{Rb}_2\text{Cu}_2\text{Mo}_3\text{O}_{12}$ [40] etc. In the frustrated FM chain, an exotic phase with short-range incommensurate spin-spin correlations is discovered by following the FM phase with moderate frustration theoretically[41] and this exotic phase has been characterized as Haldane dimer phase, which has a long-range order of dimerization, and each dimer consists of spin-triplet pair[42, 43, 44]. On the other hand, in analogy to the zigzag ladder, the FM-leg and AF-rung ladder, also indicates unconventional quantum magnetism behavior[45] and experimentally the corresponding compound is also discovered[30, 46].

Next it is natural to consider a frustrated FM ladder, where both of legs and rungs

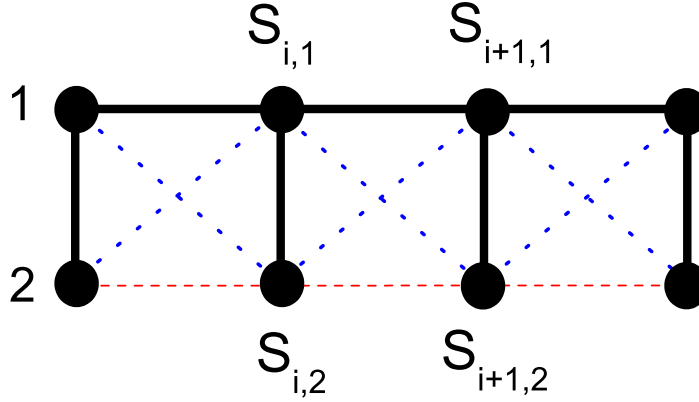


Figure 1. (Color online) The frustrated asymmetric two-leg ladder. The bold black lines denote the FM coupling, set as unity, i.e. $J_{\parallel}^1 = J_{\perp} = -1.0$. The red dashed line denotes the asymmetric FM coupling J_{\parallel}^2 . The blue diagonal dotted lines are the AF exchange $J_{\times} > 0$.

are FM, but diagonal exchange is AF. To the best of our knowledge, such the frustrated FM ladder has not been drawn too much attention. Therefore, we may ask whether or not there exists a novel ground state phase diagram in the system. Even further, one is wondering how much difference once the spin ladders are equipped with inequivalent legs (asymmetric ladders). The leg asymmetry may generate possible new phases and may induce different behaviors of the excitation spectra in the limiting cases of weak and strong asymmetries[47, 48, 49]. The fascinating models with geometric leg-asymmetry include the sawtooth strip lattice[50, 51, 52, 53], Comb-like (necklace-like) model[48] and the diamond-chain[54]. Therefore, theoretically it is attractive to investigate the frustrated asymmetric FM ladders, in particular, for highly asymmetric FM coupling in the legs and with moderate AF diagonal frustration.

The aim of this paper is to systematically study the quantum phase transition (QPT) in the frustrated asymmetric FM spin ladder. There are four ground state phases in the system: FM, partially polarized canted, spin-stripe and singlet ($S = 0$) dimerized states. At weak asymmetry, increasing NNN AF coupling can induce a first-order transition from the FM state to the spin-stripe state or to the dimerized state. At strong asymmetry, however, the processes between the FM state to the canted state and between the canted state to the spin-stripe state are second-order. The singlet dimerized state is characteristic of the $S = 0$ state with dimerization in the strong frustration regions. It is associated with the of two neighboring sites spin correlations with alternating strengths. This paper is arranged as follows. In Sec. 2, we introduce the model Hamiltonian of the two-leg frustrated asymmetric FM ladder. In Sec. 3, we firstly present the ground state phase diagram, then we introduce the physical measurements used to distinguish the QPT using the Lanczós diagonalization and the density matrix renormalization groups (DMRG) method. Sec. 4 is the summary.

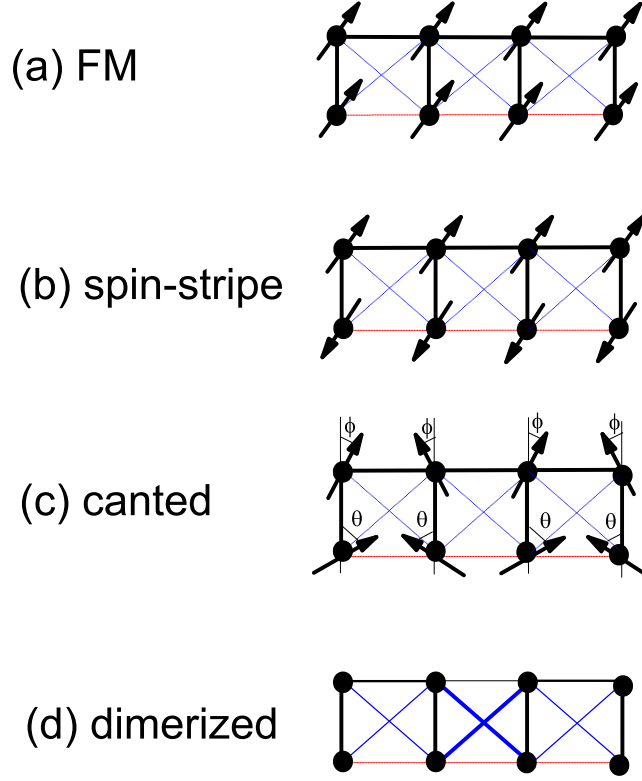


Figure 2. (Color online) The classical pictures for (a) the FM state, (b) the spin-stripe state, (c) the non-collinear canted state. (d) shows the characteristic of the alternating strengths of the spin correlations by different thickness of the bonds in the dimerized state.

2. Model and method

In this paper, we study the ground state phase diagram of the two-leg frustrated NN FM spin ladder with asymmetric legs, shown in Fig. 1. The model Hamiltonian reads as,

$$\begin{aligned}
 H = & J_{\parallel}^1 \sum_{i=1}^{L-1} \vec{S}_{i,1} \cdot \vec{S}_{i+1,1} + J_{\parallel}^2 \sum_{i=1}^{L-1} \vec{S}_{i,2} \cdot \vec{S}_{i+1,2} \\
 & + J_{\perp} \sum_{i=1}^L \vec{S}_{i,1} \cdot \vec{S}_{i,2} \\
 & + J_{\times} \sum_{i=1}^{L-1} (\vec{S}_{i,1} \cdot \vec{S}_{i+1,2} + \vec{S}_{i,2} \cdot \vec{S}_{i+1,1}),
 \end{aligned} \tag{1}$$

where $\vec{S}_{i,1}$ ($\vec{S}_{i,2}$) denotes a spin-1/2 operator of site- i on the top (bottom) leg, and L is the length of the ladder. J_{\parallel}^1 and J_{\parallel}^2 are the intraleg couplings on the top and bottom leg, respectively; J_{\perp} denotes the interleg coupling on the rungs. $J_{\parallel}^{1,2}$ and J_{\perp} are all negative, representing the NN FM exchange couplings. In addition, we introduce the diagonal AF exchange coupling $J_{\times} > 0$ between the legs. The existence of J_{\times} leads spins to align anti-parallel and competes with the $J_{\parallel}^{1,2}$, so it brings frustration. For convenience, we hereafter set $J_{\parallel}^1 = J_{\perp} = -1.0$, indicated as the bold black lines in Fig. 1. The following calculations focus on the effects of asymmetric legs and the frustration. The ratios $\alpha_a \equiv |J_{\parallel}^2/J_{\parallel}^1|$ and $\alpha_f \equiv |J_{\times}/J_{\parallel}^1|$ are defined to describe the asymmetric strength and the frustration strength, respectively.

We perform the Lanczós diagonalization [55, 56] and the density matrix renormalization group methods (DMRG) [56, 57, 58, 59, 60, 61] to study the ground state property. In contrast to the Lanczós method, the DMRG is performed with a truncated Hilbert space where the truncated basis is filtered by reduced density matrices successively. Here the number of states is kept as $m = 450$. We denote L as the ladder length so the number of sites is $N = 2 \times L$. The size of the ladder in the DMRG calculation is up to $L = 200$. We exploited the conservation of the total magnetization $\sum_i S_i^z = 0$ to achieve higher precision of the calculations. The truncation error is of the order of 10^{-7} . For the DMRG results, the open boundary conditions are used.

3. Results

Let's start from the symmetric case where $J_{\parallel}^2 = J_{\parallel}^1 = -1.0$ and consider the effects of frustration. It is well known that if there is no AF frustration, $J_{\times} = 0$, the ground state is a fully polarized FM state, where all spins align in one direction, as shown in Fig. 2(a). The total spin is $S_{\max} = 2Ls$, where $s = 1/2$. On the other hand, in the large J_{\times} limit, the spins connected by the diagonal AF bonds are anti-parallel aligned, and the ground state is singlet but has , i.e. spin aligns parallel only along the leg direction, shown in Fig. 2(b). The configuration of this spin-stripe state has also been identified in a previous paper[62]. Therefore there exists a QPT with increasing J_{\times} (the frustration strength α_f).

Then we consider a more generic case, the asymmetric ladder: $J_{\parallel}^1 \neq J_{\parallel}^2$. Numerical simulations are performed to study the ground state phase diagram in $\alpha_a - \alpha_f$ plane. When α_a is not too small ($\alpha_a \geq 0.2$), the results are similar to the symmetric case. The QPT from FM to spin-stripe is shown with increasing J_{\times} , but the boundary location may be dependent on the value of α_a . The more fascinating results are shown at strong asymmetry (as α_a is small). In addition to the FM and spin-stripe states, there exists a magnetic canted phase and a dimerized state. In the canted state, the spin orientations are non-collinear [cf. Fig. 2(c)]. Similar to the *ferrimagnetism* of mixed spin systems[63, 64, 65], magnetically it is a partially polarized ordering state, and the total spin is less than S_{\max} . On the other hand, the dimerized state shows a lone-ranged character of dimerization in spin-spin correlations along leg-1 and those along diagonal

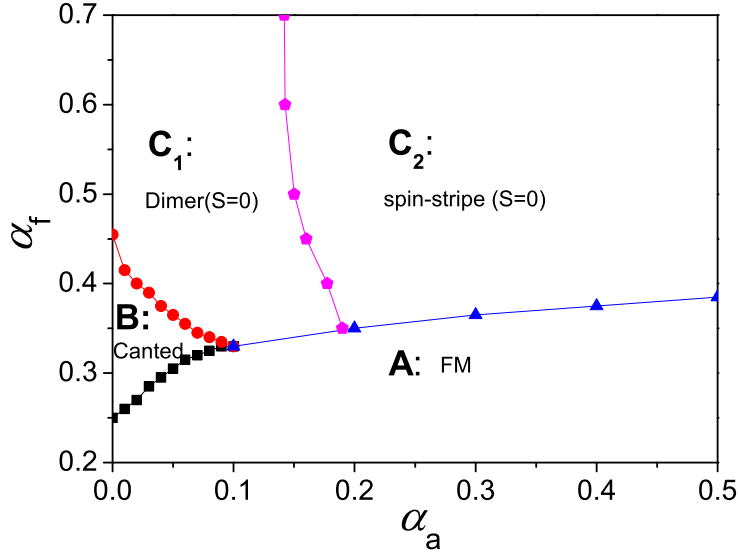


Figure 3. (Color online) The ground phase diagram in the $\alpha_a - \alpha_f$ plane, where $\alpha_a = |J_{\parallel}^2/J_{\parallel}^1|$ and $\alpha_f = |J_{\times}/J_{\parallel}^1|$ denote the asymmetry and frustration strengths, respectively. The FM state (phase **A**) and canted state (phase **B**) are magnetic. The dimerized (phase **C**₁) and the spin-stripe states (phase **C**₂) are spin singlet with $S = 0$. The phase boundaries are numerically determined by finite-size analysis in the thermodynamic limit $L = \infty$.

bonds [cf. Fig. 2(d)].

3.1. The ground state phase diagram

A first-order QPT is characterized by a finite discontinuity in the first derivative of the ground state energy. In the similar manner, a second-order QPT (or continuous QPT) is characterized by a finite discontinuity or divergence in the second derivative of the ground state energy; here we assume that the first derivative is continuous[66]. Therefore, to detect the rank of QPT in the frustrated FM ladder, one needs to calculate the ground state energy and its derivative. In addition, we also measure the local magnetization (total spin per site) and the spin correlation functions to identify the ground state phase diagram.

The thermodynamic limit phase diagram is presented in the $\alpha_a - \alpha_f$ plane in Fig. 3. The phase are determined by using the DMRG method to perform finite-size scaling. There exist four states, **A**: FM state, **B**: the canted state, **C**₁: the dimer $S = 0$ state and **C**₂: the non-dimer $S = 0$ spin-stripe state. It is interesting to find that the canted state only exists in the strong asymmetric case. At $\alpha_a = 0$, the canted state lies in the immediate frustration interval $0.25 < \alpha_f < 0.455$, while the ground state is the FM state at $\alpha_f \leq 0.25$ and the dimer phase at $\alpha_f \geq 0.455$. As α_a is lifted off the zero onset, the canted state regime shrinks gradually. When $\alpha_a \gtrsim 0.1$, the canted state

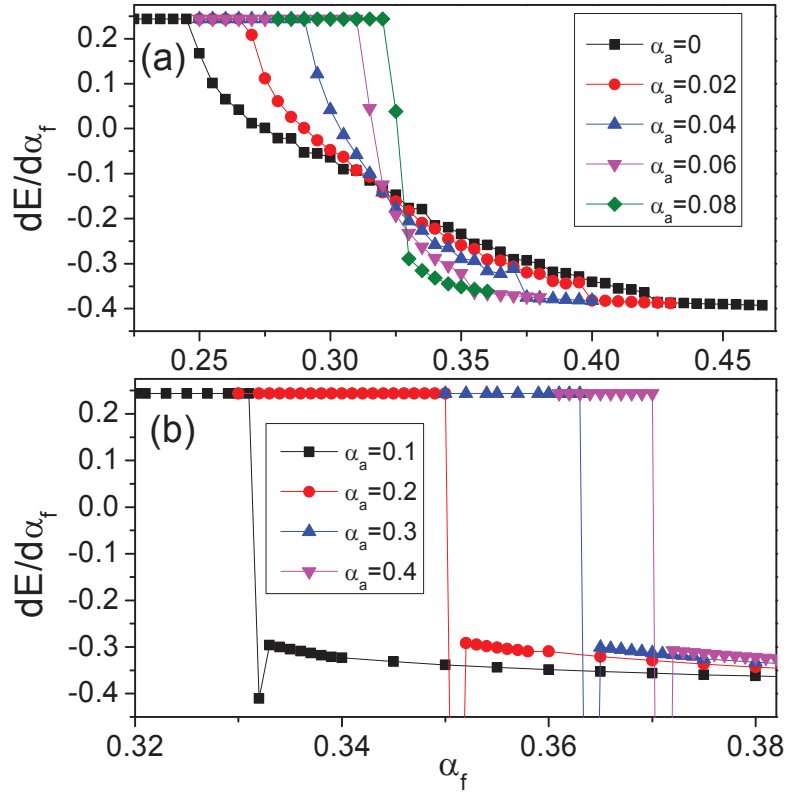


Figure 4. (Color online) The first derivative of the ground state energy $dE/d\alpha_f$ vs α_f for the $L = 40$ ladder at different asymmetric strengths α_a .

vanishes and the transition undertakes from the FM state directly to the $S = 0$ state upon increasing frustration. In the following we will present numerical evidence and analyze the corresponding pattern.

If the ground state is an FM state, the average energy per site can be exactly determined as

$$\begin{aligned}
 E &= \frac{1}{8} \left(1 - \frac{1}{L}\right) (J_{\parallel}^1 + J_{\parallel}^2 + 2J_{\times}) + \frac{1}{8} J_{\perp}, \\
 &= \frac{1}{8} \left(1 - \frac{1}{L}\right) (2\alpha_f - (\alpha_a + 1))J - \frac{1}{8} J,
 \end{aligned} \tag{2}$$

where we consider open boundary conditions. Thus, in the FM state, the first derivative of the ground state energy $dE/d\alpha_f$ is a constant.

In Figs. 4, we certainly observe the presence of the plateau on $dE/d\alpha_f$ in the small α_f regime. Thus we can identify that phase **A** is the FM state. In both Figs. 4 (a) and (b), the onsets for the plateau to collapse moves towards to larger α_f with increasing α_a . Furthermore, Fig. 4 (a) shows that for $\alpha_a \lesssim 0.1$ the energy derivatives decrease smoothly, whereas (b) shows that for $\alpha_a > 0.1$ they jump dramatically. This implies that, at small α_a (in the highly asymmetric case), the phase transition from the FM state to the phase with large α_f is second-order; otherwise it is first-order. We notice that the occurrence of the constant $dE/d\alpha_f$ collapsed has weak finite-size effect. Thus

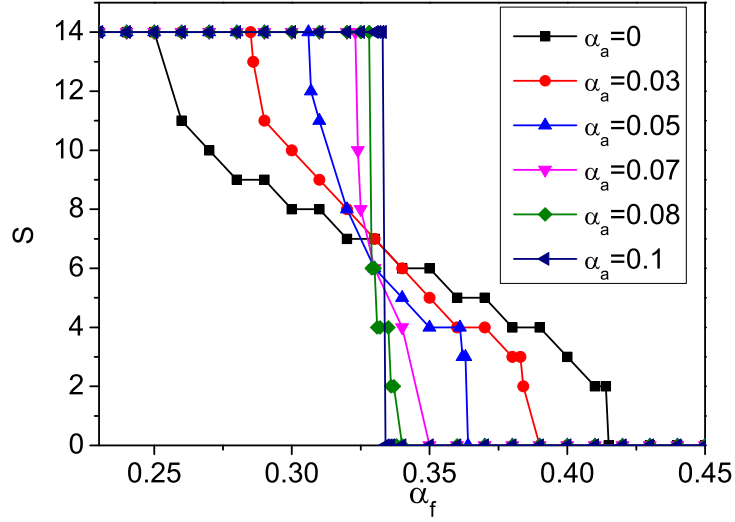


Figure 5. (Color online) The total spin S evolution as a function of α_f at different asymmetric strength α_a for the ladder system with length $L = 14$ by Lanczós diagonalization.

by small clusters, we can accurately determine the phase boundaries from phase **A** to phase **B** or to phase **C**_{1,2}.

3.2. The total spin

To further identify the magnetic nature of phase **B** and **C**, we measure the total spin S . Physically, the total spin per site is the local magnetization. The total spin is defined as

$$\langle \mathbf{S}^2 \rangle = \sum_{ij} \sum_{ab} \vec{S}_{i,a} \cdot \vec{S}_{j,b} = S(S+1). \quad (3)$$

Here we compute the total spin using Lanczós diagonalization, up to $L = 14$ with periodic boundary conditions. In Fig. 5, we can see that at small α_f , the value of S remains on $S_{\max} = Ns = L$, confirming that the ground state is fully polarized and is an FM state. Upon increasing α_f to a certain critical value, S deviates from S_{\max} , but in the small α_a regime, the total spin still remains finite. Therefore the ground state is a magnetic state but is partially polarized. This is similar to the ferrimagnetic state [63, 64, 65], which has been observed in mixed-spin systems (e.g. a spin-1/2-1 chain). In the classical analogy, we can identify that phase **B** is the canted state.

On the other side, the magnetization totally vanishes ($S = 0$) at large α_f . Thus both phase **C**_{1,2} are non-magnetic. However, the behaviors upon increasing α_f are markedly different for the strong and moderate asymmetric cases. In the small α_a regime ($\alpha_a \lesssim 0.1$), increased α_f turns the FM state (phase **A**) to the canted state (phase **B**) and then to the singlet ($S = 0$) state. Note that this procedure is subject

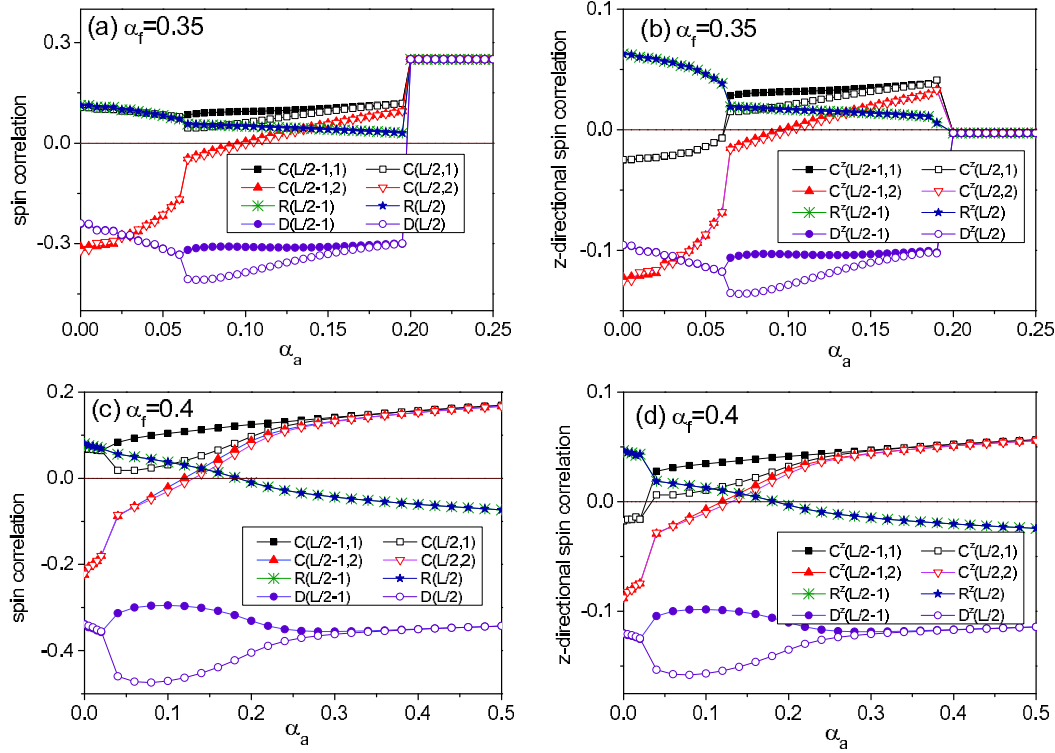


Figure 6. (Color online) The neighbor spin correlation on the middle site $l = L/2$ (hollow) and its neighbor site $l = L/2 - 1$ (solid) with $L = 48$ at (a-b) for $\alpha_f = 0.35$ and (c-d) for $\alpha_f = 0.4$. (b) and (d) depict the spin correlations along z -direction.

to the finite-size effect. Upon increasing the system size, the magnetization plateau will become smooth, and continuously decays to zero. As a consequence, the transition $\mathbf{A} \rightarrow \mathbf{B}$ and $\mathbf{B} \rightarrow \mathbf{C}_1$ can be classified as second-order. On the other hand, for $\alpha_a > 0.1$, total spin directly drops to zero, and turns to the singlet states. This characterizes a first-order transition from $\mathbf{A} \rightarrow \mathbf{C}_{1,2}$. The feature of these magnetic transitions is consistent with the previous analysis based on energy derivatives.

3.3. The spin correlations

To further investigate the ground-state properties of the diagram, in this section, we calculate the spin correlation functions. The evolution of the spin correlation results as a function of α_a at different α_f can tell us that there must be several distinct phase regimes in the parameter space.

Since our calculations are taken in the $\sum_i S_i^z = 0$ subspaces, the off-diagonal xy and diagonal z components of the spin correlations show different behavior at different phase regimes. The magnetic symmetry breaking states, canted and FM states, show that $\langle \vec{S}_i \cdot \vec{S}_j \rangle \neq 3\langle S_i^z S_j^z \rangle$. In the FM states, it can be easily deduced that all $\langle \vec{S}_i \cdot \vec{S}_j \rangle = 0.25$, but the value of $\langle S_i^z S_j^z \rangle$ can be arbitrary. However, all the zero-total-spin $S = 0$ states preserve three-dimension rotational symmetry, so $\langle \vec{S}_i \cdot \vec{S}_j \rangle = 3\langle S_i^z S_j^z \rangle$. For

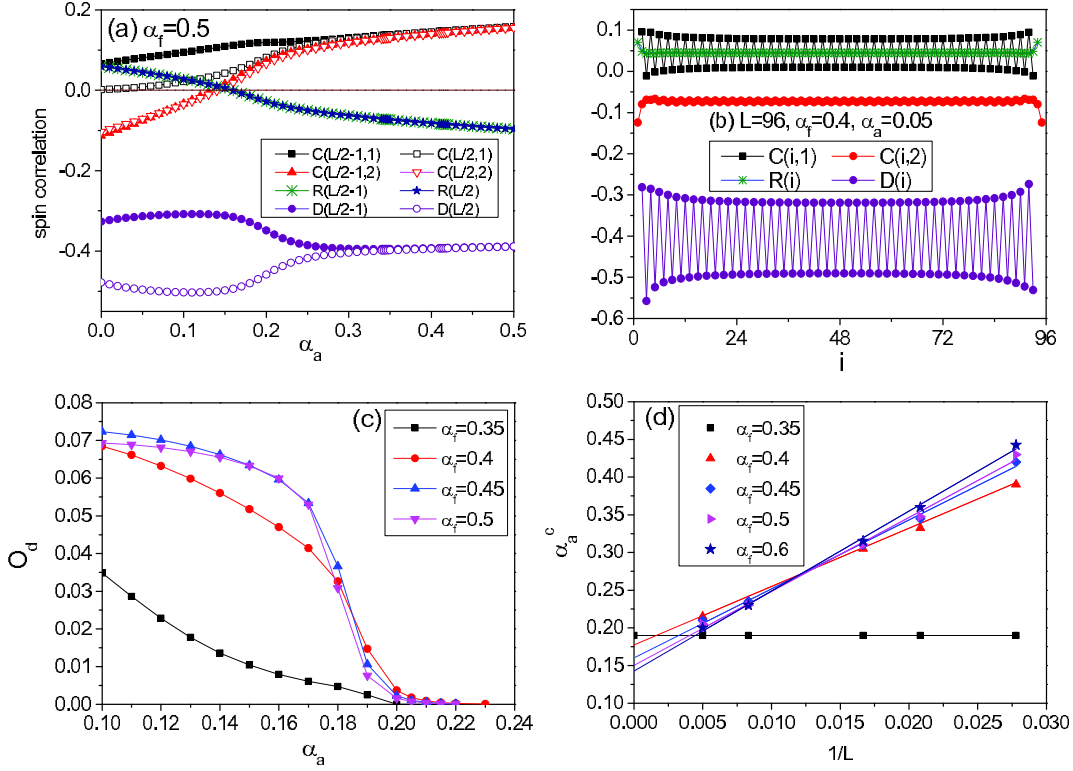


Figure 7. (Color online) (a) The neighbor spin correlation on the middle site $l = L/2$ (hollow) and its neighbor site $l = L/2 - 1$ (solid) with $L = 48$ for $\alpha_f = 0.5$. (b) The neighbor spin correlations in the entire ladder system with $L = 96$ for $\alpha_f = 0.4$ and $\alpha_a = 0.05$. (c) the dimer order parameter as a function of α_a in the $L = 200$ ladder but with different α_f values. (d) gives the scaling calculations to locate critical transition point α_a^c between the dimer state and the non-dimer state in the thermodynamic limit. The line and the zero-point values are get by linear fitting.

simplicity, the nearest neighboring spin correlations are denoted as $C(l, 1) = \langle \vec{S}_{l,1} \cdot \vec{S}_{l+1,1} \rangle$, $C(l, 2) = \langle \vec{S}_{l,2} \cdot \vec{S}_{l+1,2} \rangle$, $R(l) = \langle \vec{S}_{l,1} \cdot \vec{S}_{l,2} \rangle$ and $D(l) = \langle \vec{S}_{l,1} \cdot \vec{S}_{l+1,2} \rangle$. The corresponding correlations along z -direction are denoted as $C^z(l, 1) = \langle S_{l,1}^z S_{l+1,1}^z \rangle$, $R^z(l) = \langle S_{l,1}^z S_{l,2}^z \rangle$ and $D^z(l) = \langle S_{l,1}^z S_{l+1,2}^z \rangle$, respectively. In following correlation results, we choose the site index l as the middle site and the neighbor site, i.e. $l = L/2 - 1$ and $l = L/2$ on the $L = 48$ ladder.

Figs. 6 (a) and (c) give the spin correlation results with moderate frustration, at $\alpha_f = 0.35$ and $\alpha_f = 0.4$, while Figs. 6 (b) and (d) give their corresponding z -directional spin correlation results.

On the other hand, we can note the neighbor spin correlations in the regime with relatively weak asymmetry ($\alpha_a > 0.4$) in Figs. 6(c)-(d) and Fig. 7(a), the ground states have zero total-spin $S = 0$ and preserve the three-dimension rotational symmetry. It can be noted that when α_a is large ($\alpha_a \geq 0.4$), all $C(l, 1) = C(l, 2) > 0$, indicating FM correlation along the leg direction. On the other hand, $R(l) < 0$ and $D(l) < 0$ show AF correlation between the legs. Therefore, the system is a spin-stripe phase, where spins

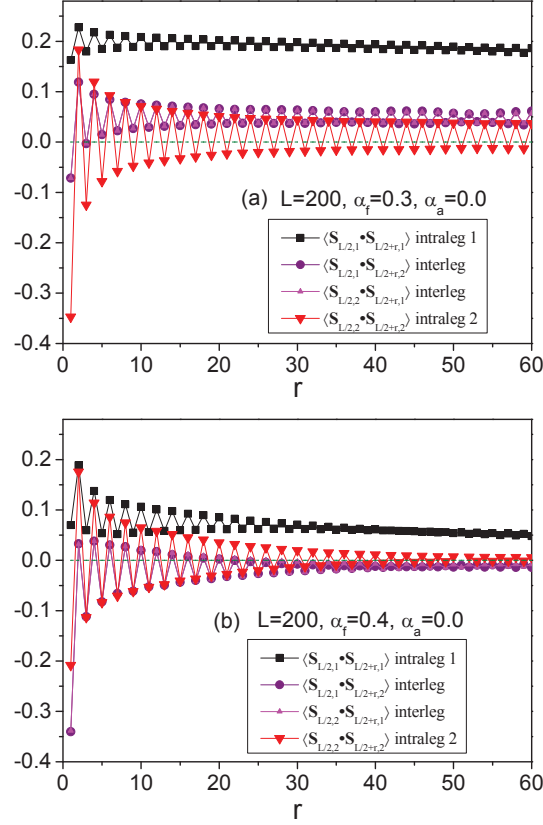


Figure 8. (Color online) The long-range spin correlations of spins in the middle rung with the other spin on the same leg and on the other leg, respectively, as a function of the distance r . The parameter of the ladder considered is $L = 200$ comb-like model ($\alpha_a = 0.0$) with different frustration strength (a) $\alpha_f = 0.3$, and (b) $\alpha_f = 0.4$.

align parallel along the leg direction, as depicted in Fig. 2(b). This state has zero spin excitation. This observation is similar to the phase I in the previous work.[62]

Interestingly, in the $S = 0$ state region, dimerization is detected at strong asymmetry. In Figs. 6(c-d) and Fig. 7(a), where $0.02 < \alpha_a < 0.3$ and $\alpha_a < 0.35$, respectively, the marked amplitude differences between $C(L/2, 1)$ (hollow) and its neighbor counterpart $C(L/2 - 1, 1)$ (solid) are observed. The dimerization patterns are also found in the diagonal correlations $D(L/2)$ and $D(L/2 - 1)$. Furthermore, Fig. 7(b) shows that the alternating strengths in spin correlations exist in the entire system. However, the nearest neighboring spin correlations on the second leg $C(L/2, 2)$ and $C(L/2 - 1, 2)$ show uniform magnitudes, or much weaker alternating behavior. These features are characteristic of the existence of dimerization on the leg-1 in the case of strong asymmetry and frustration. The dimers in leg-1 are triplet dimers with FM correlations. This state has zero spin excitation even though the spin-spin correlations in this state has an exponential decay. We would like to mention that this is different from the gapped singlet dimer state[21].

To determine the boundary of regions where the dimer phase exists, we define the dimer order parameter as $O_d = |\langle \vec{S}_{l,1} \cdot \vec{S}_{l+1,1} \rangle - \langle \vec{S}_{l+1,1} \cdot \vec{S}_{l+2,1} \rangle|$ to perform finite-size scaling analysis[17, 18, 67]. We determine the phase boundary by observing the vanishing dimer order with the criterion: $O_d < 2 \times 10^{-4}$. In Fig. 7(c), it is obvious to see that as α_a increases in the $S = 0$ regime, the dimer order parameter keeps decreasing, so there exists a critical transition point α_a^c between the dimer $S = 0$ state and the non-dimer $S = 0$ state. Fig. 7(d) shows the scaling behavior of critical transition points α_a^c at various α_f in the thermodynamic limit.

To further identify the spin arrangements of the canted states, we also calculate the long-range the correlation function of spins under different distances r [62], i.e., $C(l, l+r) = \langle \vec{S}_{l,j} \cdot \vec{S}_{l+r,j'} \rangle$, here, $j, j' = 1 (2)$ is corresponding to top (bottom) leg and r is defined as the distance between the rungs where the two spins are located. To avoid the boundary effect, we consider the inner spins of the finite chain by setting one spin in the middle rung $l = N/2$. Figs. 8 give the long range correlation functions of spins in the middle rung with the other spin on the same leg and on the other leg, respectively, as a function of the distance r . From Fig. 8(a), it can be seen that the spins on leg 1 are FM correlated while the spins on leg 2 are AF correlated, due to the strong leg asymmetry effect and the frustration effect. The long-ranged inter-leg spins are also FM correlated due to small frustration $\alpha_f = 0.3$. When the frustration strength is a little stronger, e.g., $\alpha_f = 0.4$ in Fig. 8(b), the long-ranged inter-leg spins become AF correlated. It can also be educed that the ferrimagnetic canted states for our model can not correspond to canted spiral or chiral orderings in some zigzag ladders[42, 43, 44, 68, 69] or the leg spiral spin arrangements in a previous work [62].

4. Summary

In summary, we have investigated the ground-state phases of the frustrated asymmetric spin ladder with FM nearest-neighbor interaction. In the strong asymmetric system, one can clearly distinguish three phase regimes with frustration increasing: from the pure FM state to canted state and then to $S = 0$ dimer state. On contrary, when the asymmetric strength is not strong enough, with frustration increasing there exists just one first order phase transition from FM to spin stripe state.

5. Acknowledgments

This work is supported in part of NSFC Projects No. 11404281. HHH acknowledges support from the Center for Scientific Computing at the CNSI and MRL: an NSF MRSEC (DMR-1121053) and NSF CNS-0960316.

6. Author contribution statement

All authors have contributed to the writing of the manuscript and performing the calculations.

- [1] L. Balents, *Science*, **464**, (2010) 199.
- [2] T.-H. Han, J. S. Helton, S. Chu, D. G. Nocera, J. A. Rodriguez-Rivera, C. Broholm, and Y. S. Lee, *Nature* **492**, (2012) 406.
- [3] S. Tang and J. E. Hirsch, *Phys. Rev. B* **39**, (1989) 4548.
- [4] E. Manousakis, *Rev. Mod. Phys.* **63**, (1991) 1.
- [5] E. Dagotto, *Rev. Mod. Phys.* **66**, (1994) 763.
- [6] E. Dagotto and A. Moreo, *Phys. Rev. B* **39**, (1989) 4744.
- [7] H. J. Schulz, T. A. L. Ziman, and D. Poilblanc, *J. Phys. I France* **6**, (1996) 675.
- [8] J. Richter and J. Schulenburg, *Eur. Phys. J. B* **73**, (2010) 117.
- [9] H.-C. Jiang, H. Yao, and L. Balents, *Phys. Rev. B* **86**, (2012) 024424.
- [10] P. W. Anderson, *Science* **235**, 1196 (1987).
- [11] P. A. Lee, N. Nagaosa, and X.-G. Wen, *Rev. Mod. Phys.* **78**, 17 (2006).
- [12] S. R. White, R. M. Noack, and D. J. Scalapino, *Phys. Rev. Lett.* **73**, (1994) 886.
- [13] E. Dagotto and T. M. Rice, *Science* **271**, (1996) 618.
- [14] M. Uehara, T. Nagata, J. Akimitsu, H. Takahashi, N. Mori, and K. Kinoshita, *J. Phys. Soc. Jpn.* **65**, (1996) 2764.
- [15] X. Wang, *Mod. Phys. Lett. B* **14**, (2000) 327.
- [16] O. A. Starykh and L. Balents, *Phys. Rev. Lett.* **93**, 127202 (2004).
- [17] G. Fáth, O. Legeza, and J. Sólyom, *Phys. Rev. B* **63**, (2001) 134403.
- [18] H. -H. Hung, C.-D. Gong, Y.-C. Chen, and M. -F. Yang, *Phys. Rev. B* **73**, (2006) 224433.
- [19] T. Hakobyan, *Phys. Rev. B* **75**, (2007) 214421.
- [20] B. W. Ramakko and M. Azzouz, *Phys. Rev. B* **76**, (2007) 064419.
- [21] G. -H. Liu, H. -L. Wang, and G. -S. Tian, *Phys. Rev. B* **77**, (2008) 214418.
- [22] E. H. Kim, O. Legeza, and J. Sólyom, *Phys. Rev. B* **77**, (2008) 205121.
- [23] T. Hikihara and O. A. Starykh, *Phys. Rev. B* **81**, (2010) 064432.
- [24] S. Dong, W. Rui, L. Guang-Hua, and T. Guang-Shan, *Chinese Phys. B* **19**, (2010) 077503.
- [25] . W. Rui, L. Guang-Hua, and T. Guang-Shan, *Commun. Theor. Phys.* **55**, (2011) 1102.
- [26] T. Barnes, E. Dagotto, J. Riera, and E. S. Swanson, *Phys. Rev. B* **47**, (1993) 3196.
- [27] T. Tonegawa and I. Harada, *J. Phys. Soc. Jpn.* **58**, (1989) 2902.
- [28] E. Plekhanov, A. Avella, and F. Mancini, *Eur. Phys. J. B* **77**, (2010) 381.
- [29] R. Bursill, G. A. Gehring, D. J. J. Farnell, J. B. Parkinson, T. Xiang, and C. Zeng, *J. Phys.: Condens. Matter* **7**, (1995) 8605.
- [30] T. Vekua, A. Honecker, H.-J. Mikeska, and F. Heidrich- Meisner, *Phys. Rev. B* **76**, (2007) 174420.
- [31] F. Heidrich-Meisner, A. Honecker, and T. Vekua, *Phys. Rev. B* **74**, (2006) 020403.
- [32] F. Heidrich-Meisner, I. P. McCulloch, and A. K. Kolezhuk, *Phys. Rev. B* **80**, (2009) 144417.
- [33] T. Hikihara, L. Kecke, T. Momoi, and A. Furusaki, *Phys. Rev. B* **78**, (2008) 144404.
- [34] J. Sudan, A. Lüscher, and A. M. Läuchli, *Phys. Rev. B* **80**, (2009) 140402.
- [35] K. Hida, K. Takano, and H. Suzuki, *J. Phys. Soc. Jpn.* **82**, (2013) 064703.
- [36] R. Jafari and A. Langari, *Phys. Rev. B* **76**, (2007) 014412.
- [37] H. T. Lu, Y. J. Wang, S. Qin, and T. Xiang, *Phys. Rev. B* **74**, 134425 (2006).
- [38] S. L. Drechsler, J. Richter, A. A. Gippius, A. Vasiliev, A. A. Bush, A. S. Moskvina, J. Malek, Y. Prots, W. Schnelle, and H. Rosner, *Europhys. Lett* **73**, (2006) 83.
- [39] M. Enderle, C. Mukherjee, B. Fak, R. K. Kremer, J.-M. Broto, H. Rosner, S.-L. Drechsler, J. Richter, J. Malek, A. Prokofiev, et al., *Europhys. Lett.* **70**, (2005) 237.
- [40] M. Hase, H. Kuroe, K. Ozawa, O. Suzuki, H. Kitazawa, G. Kido, and T. Sekine, *Phys. Rev. B* **70**, (2004) 104426.
- [41] J. Sirker, V. Y. Krivnov, D. V. Dmitriev, A. Herzog, O. Janson, S. Nishimoto, S.-L. Drechsler,

- and J. Richter, Phys. Rev. B **84**, (2011) 144403.
- [42] S. Furukawa, M. Sato, and A. Furusaki, Phys. Rev. B **81**, (2010) 094430.
 - [43] S. Furukawa, M. Sato, and S. Onoda, Phys. Rev. Lett. **105**, (2010) 257205.
 - [44] S. Furukawa, M. Sato, S. Onoda, and A. Furusaki, Phys. Rev. B **86**, (2012) 094417.
 - [45] G. I. Japaridze, A. Langari, and S. Mahdavi, J. Phys.: Condens. Matter **19**, (2007) 076201.
 - [46] H. Yamaguchi, K. Iwase, T. Ono, T. Shimokawa, H. Nakano, Y. Shimura, N. Kase, S. Kittaka, T. Sakakibara, T. Kawakami, et al., Phys. Rev. Lett. **110**, (2013) 157205.
 - [47] S. Chen, H. Büttner, and J. Voit, Phys. Rev. Lett. **87**, (2001) 087205.
 - [48] F. H. L. Essler, T. Kuzmenko, and I. A. Zaliznyak, Phys. Rev. B **76**, (2007) 115108.
 - [49] D. N. Aristov, C. Brunger, F. F. Assaad, M. N. Kiselev, A. Weichselbaum, S. Capponi, and F. Alet, Phys. Rev. B **82**, 174410 (2010).
 - [50] D. Sen, B. S. Shastry, R. E. Walstedt, and R. Cava, Phys. Rev. B **53**, (1996) 6401.
 - [51] T. Nakamura and K. Kubo, Phys. Rev. B **53**, (1996) 6393.
 - [52] T. Nakamura and S. Takada, Phys. Rev. B **55**, (1997) 14413.
 - [53] D. V. Dmitriev, V. Ya. Krivnov, J. Phys.: Condens. Matter **28**, (2016) 506002.
 - [54] K. Okamoto, T. Tonegawa, Y. Takahashi, and M. Kaburagi, J. Phys. Condens. Matter **11**, 10485 (1999).
 - [55] H. Q. Lin, Phys. Rev. B **42**, (1990) 6561.
 - [56] A. L. Malvezzi, Brazilian J. of Phys. **33**, (2003) 55.
 - [57] S. R. White, Phys. Rev. Lett. **69**, (1992) 2863.
 - [58] S. R. White, Phys. Rev. B **48**, (1993) 10345.
 - [59] S. R. White, Physics Report **301**, (1998) 187.
 - [60] N. Shibata, J. Phys. A: Math. Gen **36**, (2003) R381.
 - [61] U. Schollwöck, Rev. Mod. Phys. **77**, (2005) 259.
 - [62] Y. C. Li and H. Q. Lin, New J. Phys. **14**, (2012) 063019.
 - [63] S. K. Pati, S. Ramasesha, and D. Sen, Phys. Rev. B **55**, (1997) 8894.
 - [64] C. Wu, B. Chen, X. Dai, Y. Yu, and Z.-B. Su, Phys. Rev. B **60**, (1999) 1057.
 - [65] N. B. Ivanov and J. Richter, Phys. Rev. B **69**, (2004) 214420.
 - [66] L. E. Reichl, A Modern Course in Statistical Physics (John Wiley and Sons, New York, 1998).
 - [67] H. -H. Hung, Y. Wang, C. D. Batista and C. Wu, Phys. Rev. B **84**, (2011) 054406.
 - [68] C. D. Batista, Phys. Rev. B **80**, (2009) 180406.
 - [69] K. Okunishi, J. Phys. Soc. Jpn. **77**, (2008) 114004.